

## Force balance and ion particle transport differences in high and low confinement tokamak edge pedestals

W. M. Stacey and R. J. Groebner

Citation: [Physics of Plasmas](#) **17**, 112512 (2010); doi: 10.1063/1.3520067

View online: <http://dx.doi.org/10.1063/1.3520067>

View Table of Contents: <http://scitation.aip.org/content/aip/journal/pop/17/11?ver=pdfcov>

Published by the [AIP Publishing](#)

---

### Articles you may be interested in

[Effect of non-diffusive processes on transport and its interpretation in the tokamak plasma edge](#)

[Phys. Plasmas](#) **20**, 112503 (2013); 10.1063/1.4829433

[Interpretation of changes in diffusive and non-diffusive transport in the edge plasma during pedestal buildup following a low-high transition in DIII-D](#)

[Phys. Plasmas](#) **20**, 012509 (2013); 10.1063/1.4775601

[The pinch of cold ions from recycling in the tokamak edge pedestal a\)](#)

[Phys. Plasmas](#) **18**, 056116 (2011); 10.1063/1.3589467

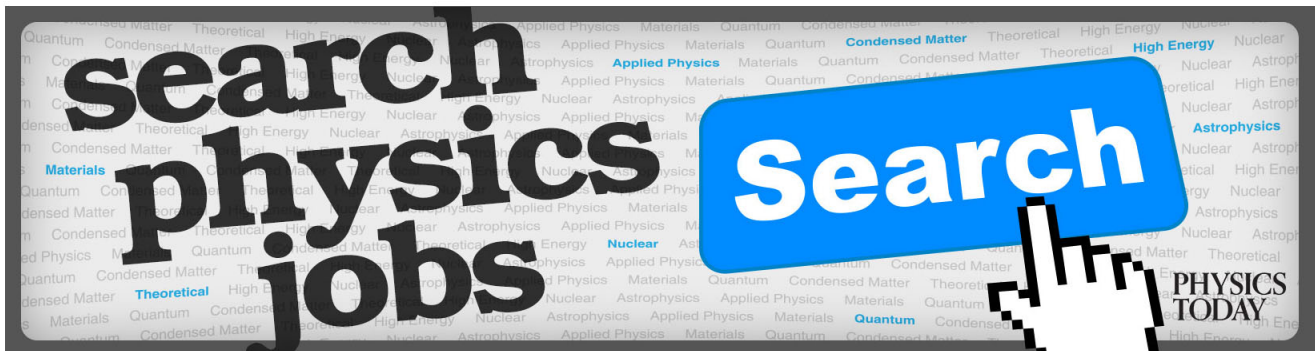
[Interpretation of particle pinches and diffusion coefficients in the edge pedestal of DIII-D H-mode plasmas](#)

[Phys. Plasmas](#) **16**, 102504 (2009); 10.1063/1.3241698

[Wall intersection of ion orbits induced by fast transport of pedestal plasma over an electrostatic potential hill in a tokamak plasma edge](#)

[Phys. Plasmas](#) **12**, 102501 (2005); 10.1063/1.2052487

---



# Force balance and ion particle transport differences in high and low confinement tokamak edge pedestals

W. M. Stacey<sup>1</sup> and R. J. Groebner<sup>2</sup>

<sup>1</sup>Georgia Institute of Technology, Atlanta, Georgia 30332, USA

<sup>2</sup>General Atomics, San Diego, California 92186, USA

(Received 2 September 2010; accepted 3 November 2010; published online 22 November 2010)

The various terms in the radial force balance in the edge plasma are evaluated using experimental data from the low (L) and high (H) confinement phase of a DIII-D [J. Luxon, Nucl. Fusion **42**, 614 (2002)] discharge in order to investigate the differences in the radial force balance among the several electromagnetic and pressure gradient forces in L-mode and H-mode. The roles of cross-field toroidal momentum transport and of a radial pinch velocity in determining different radial particle fluxes in L-mode and H-mode are elucidated. © 2010 American Institute of Physics. [doi:10.1063/1.3520067]

## I. INTRODUCTION

One of the most visible differences in the data between low confinement (L-mode) and high confinement (H-mode) tokamak plasmas is the structure of the density and temperature profiles in the plasma edge. In L-mode plasmas, the density and temperature profiles decrease rather gradually from the plasma core through the edge to the last closed flux surface (LCFS), while H-mode plasmas exhibit density and temperature profiles that are relatively flat from the core out through much of the plasma edge but then drop sharply just inside the LCFS, forming as such an “edge pedestal” in the density and temperature profiles.<sup>1,2</sup> If diffusive processes govern particle (heat) transport, a reduction in particle (heat) diffusion coefficient in the steep-gradient edge pedestal location would be required in order to remove the particle (heat) flux passing out of the core plasma and across the LCFS. Using the diffusive relationship and measured density gradients, the inferred profiles of particle (heat) diffusion coefficients naturally exhibit a dip in the steep-gradient region, giving rise to concept of an edge “transport barrier.” However, in some cases,<sup>3</sup> the inferred particle diffusion coefficients are quite small ( $D \ll 0.1 \text{ m}^2/\text{s}$ ), occasionally even smaller than the inherent neoclassical level, implying that a purely diffusive representation of the ion radial particle flux neglects some important phenomena.

The profiles of radial electric field and plasma rotation velocity are also observed<sup>4</sup> to differ between L-mode and H-mode plasmas. This indicates that the balance between radial electric,  $V \times B$ , and pressure gradient forces must be different as well in L-mode and H-mode edge pedestals.

We have recently presented<sup>5,6</sup> a methodology for the evaluation of the radial force balance almost entirely from measured data without resort to theoretical models other than momentum and particle balance. The derivation of this methodology yields a “pinch-diffusion” relation for the radial particle flux as a natural consequence of momentum balance.

There have been suggestions of a particle pinch since the earliest days of tokamak research.<sup>7</sup> Detailed numerical modeling<sup>8</sup> of DIII-D (Ref. 9) discharges has needed to use a pinch in order to obtain reasonable agreement with experi-

ment, and more recent interpretive calculations<sup>10</sup> of DIII-D have inferred an inward particle flux early in the H-mode phase. The experimental observation<sup>11</sup> of pedestal density width increasing with time on DIII-D may also be attributed to an inward pinch. On the theoretical side, at least one well-developed transport theory (paleoclassical) predicts<sup>3</sup> a pinch-diffusion form for the radial particle flux.

Research on the H-mode plasma edge is an important topic both because of the scientific challenge of understanding the H-mode pedestal and due to a need to develop improved confidence in predictions of pedestal height in International Thermonuclear Experimental Reactor. The overview paper<sup>12</sup> of the recent 12th International Workshop on H-Mode Physics and Transport Barriers organized the recent research into the following categories: (1) *scaling of the pedestal width and implications for pedestal width models*, including studies of scaling with  $\rho^*$  (e.g., Refs. 13 and 14) and with  $\beta_\theta^{1/2}$  (e.g., Refs. 15–18); (2) *dynamics of pedestals with Type-I ELMs*, including studies of the magnetohydrodynamic stability limit and time evolution of the edge current density (e.g., Refs. 19 and 20), studies of ELM crashes (e.g., Refs. 21 and 22), studies of ELM recovery (e.g., Refs. 11, 23, and 24), and studies of small and no ELM regimes (e.g., Refs. 25–28); and *pedestal transport* (e.g., Ref. 29).

The present paper falls into the category of particle transport in the pedestal, but it also presents a new force balance interpretation of pedestal structure (width and height) in the absence of effects due to ELMs. A significant increase in the edge density gradient and edge density has long been known to be an important characteristic of the L-H transition. In the context of purely diffusive particle transport models, this formation of a density pedestal has been interpreted in terms of a reduction in the diffusion coefficient, i.e., as a transport barrier. The present paper uses a pinch-diffusion model for the radial particle flux, as is required by momentum balance, and evaluates both the diffusion coefficient and pinch velocity from experimental data. It is found that a large increase in the inward pinch velocity, rather than a large decrease in diffusion coefficient, characterizes the H-mode plasma edge relative to the L-mode. The types of

radial electric field and rotation profiles associated with this large inward pinch force have long been known experimentally to be characteristic of H-mode but have generally been interpreted as causing a shear stabilization of turbulence due to microinstabilities leading to a reduction in the particle (and heat) diffusion coefficient. Thus, this paper presents a radically new interpretation of the reasons for the observed differences in L-mode and H-mode edge pedestals.

## II. RADIAL FORCE BALANCE, PINCH VELOCITY, AND DIFFUSION COEFFICIENT

The toroidal and radial momentum balance equations may be written for any ion species “ $j$ ,”

$$n_j m_j [(\nu_{jk} + \nu_{dj})V_{\phi j} - \nu_{jk}V_{\phi k}] = n_j e_j E_\phi^A + n_j e_j B_\theta V_{rj} + M_{\phi j} \quad (1)$$

and

$$V_{\phi j} = \frac{1}{B_\theta} \left[ E_r + V_{\theta j} B_\phi - \frac{1}{n_j e_j} \frac{\partial p_j}{\partial r} \right], \quad (2)$$

where “ $k$ ” in general refers to a sum over other ion species. In this paper,  $j$  will refer to deuterium and  $k$  to carbon in a two-species model. The quantity  $\nu_{dj}$  is a toroidal angular

momentum transfer frequency, which represents the combined effect of viscosity, inertia, atomic physics, and other “anomalous” processes. Justification for representing the toroidal momentum transfer processes in this form is discussed in Ref. 30.  $M_{\phi j}$  is the toroidal momentum input,  $e_j$  refers to the charge of species  $j$ , and the other symbols have their usual meaning.

Equations (1) and (2) may be combined<sup>5,6</sup> to obtain a pinch-diffusion relation for the main ion radial particle flux,

$$\begin{aligned} \Gamma_j &\equiv n_j V_{rj} = - \frac{n_j \hat{D}_j}{p_j} \frac{\partial p_j}{\partial r} + n_j V_{rj}^{\text{pinch}} \\ &= - \hat{D}_j \left( \frac{\partial n_j}{\partial r} + \frac{n_j}{T_j} \frac{\partial T_j}{\partial r} \right) + n_j V_{rj}^{\text{pinch}}, \end{aligned} \quad (3)$$

where the diffusion coefficient is

$$\hat{D}_j \equiv \frac{m_j T_j \nu_{jk}}{(e_j B_\theta)^2} \left( 1 + \frac{\nu_{dj}}{\nu_{jk}} - \frac{e_j}{e_k} \right) \quad (4)$$

and

$$V_{rj}^{\text{pinch}} \equiv \frac{[-M_{\phi j} - n_j e_j E_\phi^A + n_j m_j (\nu_{jk} + \nu_{dj})(f_p^{-1} V_{\theta j} + E_r/B_\theta) - n_j m_j \nu_{jk} V_{\phi k}]}{n_j e_j B_\theta} \quad (5)$$

is identified as a “velocity pinch,” where  $f_p \equiv B_\theta/B_\phi$ . Thus, momentum balance requires radial particle transport to be of a “pinch-diffusive” nature. The external momentum input, which is a small term in Eq. (5) in the edge, can be calculated from the known beam geometry and power input. The induced toroidal electric field, which is also a small term, can be determined from the measured loop voltage. The density, temperature, radial electric field, and carbon ( $k$ ) toroidal rotation velocity are measured, and  $\nu_{jk}$  can be calculated using the measured density and temperature.

Since the deuterium rotation velocities are not measured, we make use of a perturbation analysis<sup>5,6</sup> in which  $(V_{\phi j} - V_{\phi k})$  is taken as a small parameter to derive expressions, which may be used to evaluate the experimental deuterium ( $j$ ) and carbon ( $k$ ) toroidal angular momentum transfer frequencies for the main ions,

$$\nu_{dj} = \frac{(n_j e_j E_\phi^A + e_j B_\theta \Gamma_j + M_{\phi j}) + (n_k e_k E_\phi^A + e_k B_\theta \Gamma_k + M_{\phi k})}{(n_j m_j + n_k m_k) V_{\phi k}^{\text{exp}}} \quad (6)$$

and for the carbon impurity ions

$$\nu_{dk} = \frac{(n_k e_k E_\phi^A + e_k B_\theta \Gamma_k + M_{\phi k}) + n_j m_j \nu_{jk} (V_{\phi j} - V_{\phi k})_0}{n_k m_k V_{\phi k}^{\text{exp}}}, \quad (7)$$

where

$$(V_{\phi j} - V_{\phi k})_0 = \frac{(n_j e_j E_\phi^A + e_j B_\theta \Gamma_j + M_{\phi j}) - n_j m_j \nu_{dj} V_{\phi k}^{\text{exp}}}{n_j m_j (\nu_{jk} + \nu_{dj})} \quad (8)$$

is the first order perturbation estimate of the difference in deuterium and carbon toroidal rotation velocities. Evaluation of Eq. (8) using the data for DIII-D discharge 118897 analyzed in this paper reveals that this difference is in fact small compared to the measured carbon rotation, confirming the validity of the perturbation analysis.

The values of the radial particle fluxes needed to evaluate these equations were obtained by solving the continuity equation, using the measured densities and temperatures and calculated neutral beam and recycling neutral sources, as described in many of our recent papers, e.g., Ref. 10. These calculations involved global particle and power balances to determine heat and particle fluxes across the separatrix into the scrape-off layer, a two-point divertor calculation of the fluxes of heat and ions to the targets, and a two-dimensional transport calculation of the neutral atoms recycling from the divertor targets and chamber wall back across the separatrix

to fuel the plasma. These calculations were benchmarked to experimental measurements (e.g., density and temperature at the midplane separatrix, radiation from the core and divertor, and confinement time).

Thus, the only quantity in the above equations that cannot be evaluated from measured or otherwise known data is the deuterium poloidal rotation velocity. A neoclassical calculation<sup>5</sup> predicts that the deuterium and carbon poloidal rotation velocities in the H-mode phase of the shot examined in this paper have a similar profile and magnitude, but both are predicted to be more positive (or less negative) than the measured carbon poloidal rotation velocity. Other calculations have found a similar result.<sup>31–33</sup> However, this result cannot be generalized because dominance of the poloidal viscous force over the friction force will cause the two species to rotate in opposite directions, while the dominance of the friction force over the viscous force will cause the two species to rotate in the same direction. In fact, a measurement<sup>34</sup> in a DIII-D helium plasma with carbon impurities found the two species to be rotating in opposite directions, and a trace impurity neoclassical calculation<sup>34</sup> confirmed this result. In this paper, we will use the measured carbon poloidal rotation velocity to evaluate the deuterium poloidal rotation term in the pinch velocity. We believe on the basis of neoclassical calculations<sup>5</sup> that this assumption may be close to correct, but, in any case, it leads to a conservative lower bound on the magnitude of the pinch velocity, as discussed in Appendix A.

We note that it has been assumed that the logarithmic gradient of the carbon and deuterium pressures are the same to reduce Eqs. (1) and (2) to Eqs. (3)–(5). The observed experimental carbon to deuterium density ratio is relatively flat in the edge region, and the collisionality is sufficient that the carbon and deuterium temperatures should be the same, so this should be a good approximation for the shot examined in this paper. In cases where this approximation cannot be made, two coupled pinch-diffusion relations with separate diffusion coefficients and pinch velocities are obtained for the carbon and deuterium ions.<sup>30</sup>

We further note that Eqs. (3)–(5) are required by momentum balance. This means that the common practice of implicitly assuming a purely diffusive particle flux (i.e., using diffusion theory) and making an *ad hoc* choice of diffusion coefficient either to match experimental profiles or based on some theory for particle transport is generally inconsistent with momentum conservation. First principles transport theory would enter Eqs. (3)–(5) via the determination of the angular momentum transport frequencies  $\nu_{dj}$  and  $\nu_{dk}$ , rather than determining them experimentally, as is done in this paper.

### III. EVALUATION OF VPINCH AND D IN THE L-MODE AND H-MODE PHASES OF A DIII-D DISCHARGE

Discharge #118897 was a conventional H-mode discharge with a long H-mode phase with low heating power to delay the onset of edge-localized modes (ELMs). The above expressions for the momentum transfer frequency, the ion-impurity collision frequency, the pinch velocity, and the dif-

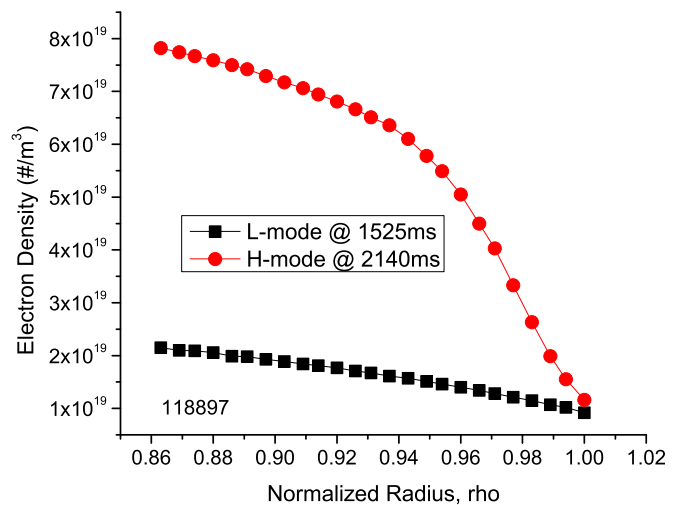


FIG. 1. (Color online) Fitted experimental electron density (Thomson) in shot #118897.

fusion coefficient were evaluated for both the L-mode phase (1525 ms) and the ELM-free H-mode phase (2140 ms) of DIII-D discharge 118897. We have previously documented<sup>10</sup> the experimental time history and calculated particle and heat fluxes for this discharge. The density and temperature data and their measurement and fitting are described in Refs. 5 and 10, and the fitted data are given in Figs. 1–6.

The experimental toroidal momentum transfer frequencies inferred for the deuterium main ions by using the measured data to evaluate Eq. (6) are given in Fig. 7. Similar frequencies were inferred for the carbon impurity ions by using the measured data to evaluate Eqs. (7) and (8). The ion-impurity (D-C) collision frequency is also shown in Fig. 7. Clearly, momentum exchange due to cross-field transport processes ( $\nu_{dj}$ ) is more important than collisional momentum exchange ( $\nu_{jk}$ ) in the steep-gradient edge pedestal region, but not in the flattop region, of the plasma edge.

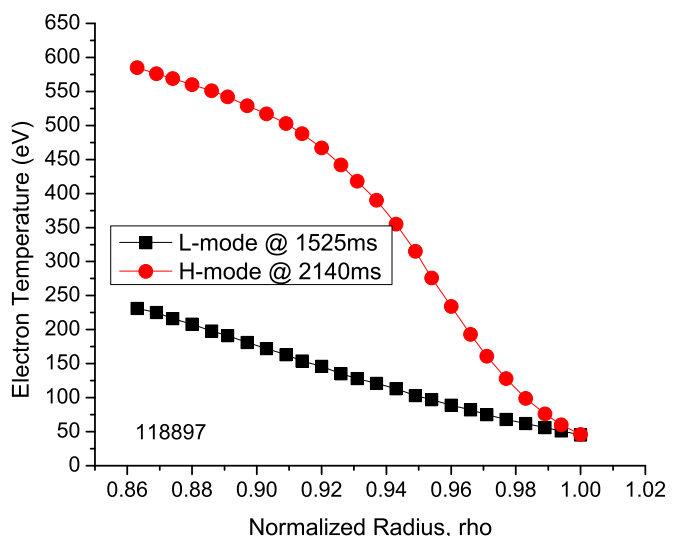


FIG. 2. (Color online) Fitted experimental electron temperature (Thomson) in shot #118897.



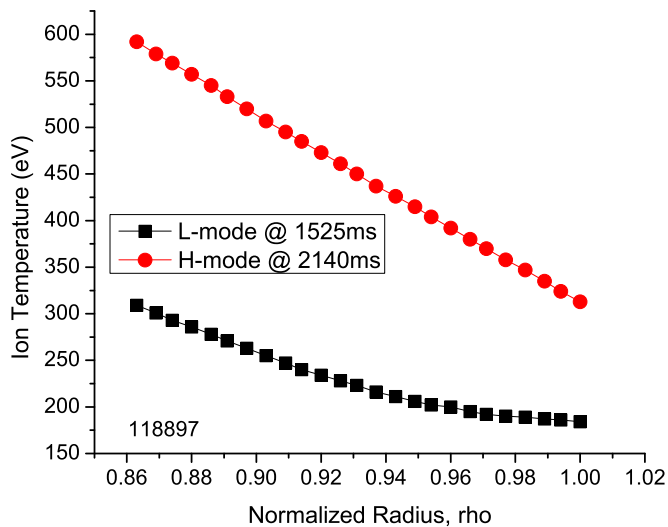


FIG. 3. (Color online) Fitted experimental ion temperature (CER) in shot #118897.

Using these inferred experimental momentum transfer frequencies and the measured densities and temperatures, the deuterium particle diffusion coefficients shown in Fig. 8 were evaluated. Whereas the L-mode diffusion coefficient increased dramatically as the separatrix was approached, the H-mode diffusion coefficient was almost uniform across the edge region, excepting an order of 20% dip in the steep-gradient region of  $0.96 < \rho < 1.0$ .

Note that it is the interplay of the momentum transfer and interspecies collision frequencies shown in Fig. 7 and the temperature profiles shown in Fig. 3 that produced the dip in the H-mode diffusion coefficient calculated from Eq. (4) and shown in Fig. 8. The stabilization of microinstabilities<sup>35,36</sup> associated with the strong shearing of radial electric field and/or poloidal rotation velocity shown in Figs. 4 and 5 for the H-mode discharge is widely thought to account for such dips in the particle (and heat) diffusion coefficients observed in the interpretation of H-mode discharges with diffusive or conductive transport models. Such

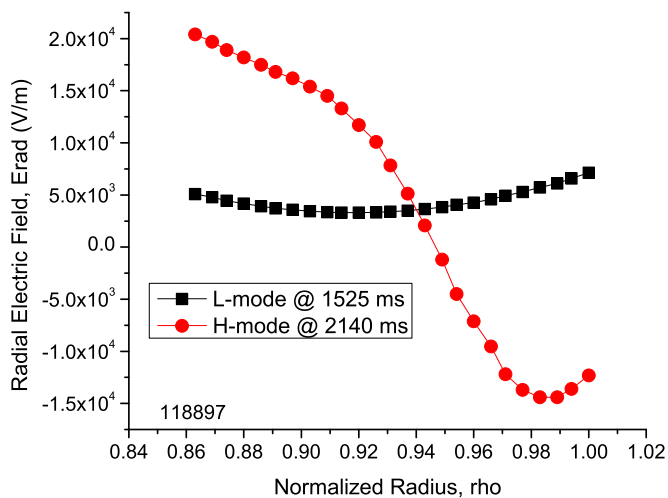


FIG. 4. (Color online) Fitted experimental radial electric field (from carbon momentum balance) in shot #118897.

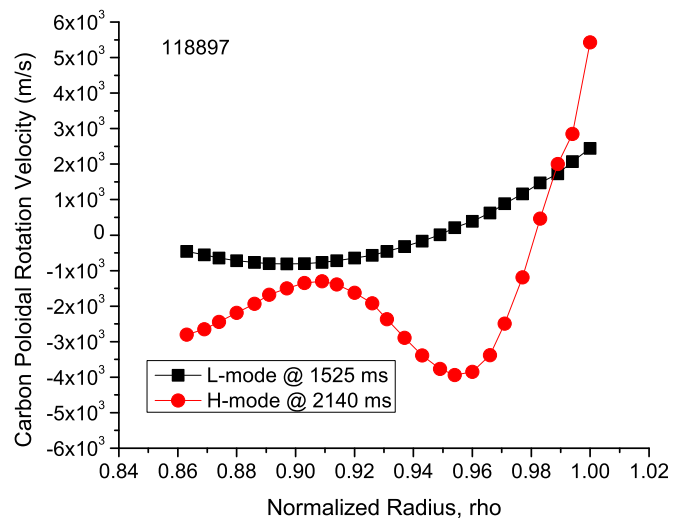


FIG. 5. (Color online) Fitted experimental carbon poloidal rotation velocity (CER) in shot #118897. (The positive toroidal direction is defined as the direction of the plasma current, and the positive sign of the poloidal velocity is taken in the right-hand  $r-\theta-\phi$  system sense. In shot #118897, the positive poloidal direction is down at the outboard midplane.)

shear stabilization phenomena would enter the interpretive methodology of this paper through the experimentally inferred momentum transfer frequencies ( $\nu_{dj}$ ). However, the H-mode momentum transfer frequency shown in Fig. 7 increases sharply in the steep-gradient region, rather than decreasing as would be expected from shear stabilization of anomalous transport.

The deuterium pinch velocities evaluated by using measured data in Eq. (5) are plotted in Fig. 9 for the L-mode phase and in Fig. 10 for the H-mode phase. It is important to realize that the pinch velocities are normalized forces and that Eq. (5) is a force balance equation. The contributions of the individual rotation and radial electric field terms are also shown. The contributions due to the induced toroidal electric field ( $E_{\phi}^A$ ) and to the neutral beam momentum input ( $M_{\phi j}$ ) were small. In the L-mode phase of Fig. 9, the  $E_{\text{rad}}$  and  $V_{\theta}$

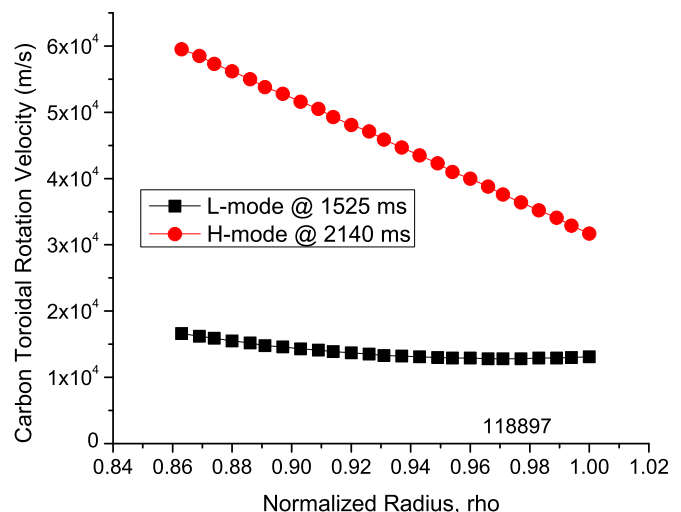


FIG. 6. (Color online) Fitted experimental carbon toroidal rotation velocity (CER) in shot #118897.

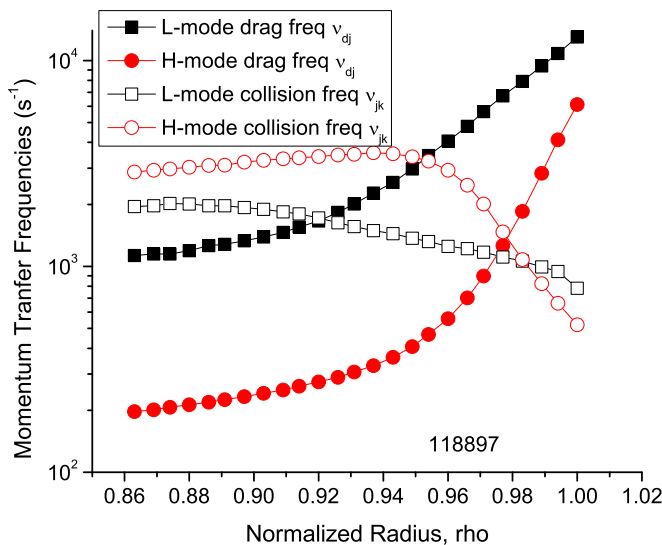


FIG. 7. (Color online) Inferred experimental momentum transfer drag frequency and D-C collision frequency in shot #118897.

contributions cancel in the edge pedestal and the radial “pinch” velocity (the net combination of electromagnetic forces) is small but outward over the plasma edge (the net outward pinch may result from approximations, but the small magnitude is the important point). On the other hand, in the H-mode phase the electric field has changed signs, and the  $E_{\text{rad}}$  and  $V_{\theta}$  contributions combine to produce a large inward pinch velocity (net electromagnetic force) in the edge pedestal.

The net radial particle flux required by radial force balance is given by Eq. (3). There is a large inward net electromagnetic component (the pinch velocity term) in the H-mode phase. In the L-mode phase, the net electromagnetic force is smaller (because of cancellation) and outward.

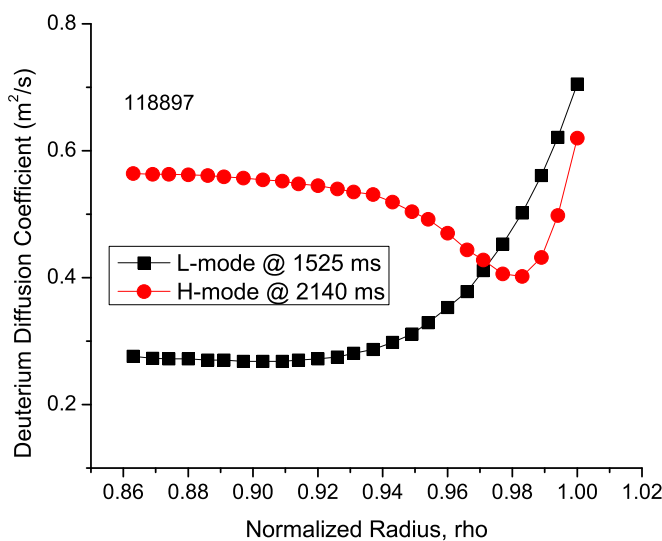


FIG. 8. (Color online) Deuterium diffusion coefficient constructed from experimental data for shot #118897.

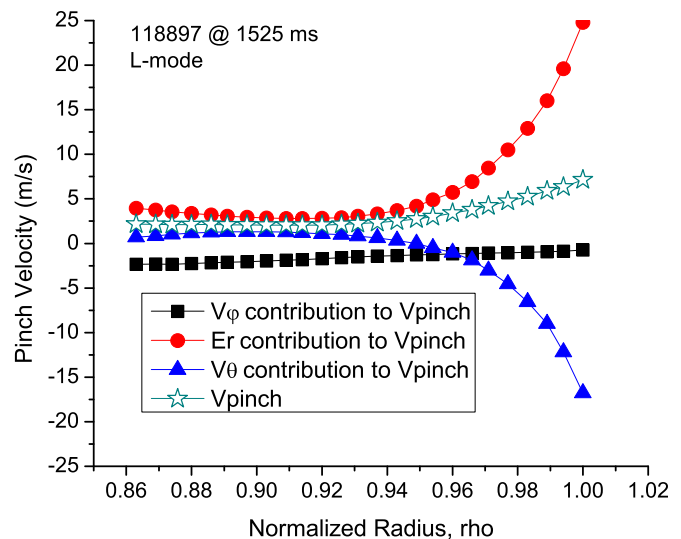


FIG. 9. (Color online) Inferred experimental pinch velocity in L-mode phase of shot #118897.

#### IV. DISCUSSION

The evaluation of the radial force balance in the edge plasma using measured data reveals that there is a major difference in the radial particle pinch between L-mode and H-mode, in the shot analyzed, that could account for why the H-mode density profile is dramatically different than the L-mode profile. This difference in the pinch is related to differences between L-mode and H-mode in  $E_{\text{rad}}$  and the poloidal rotation velocity in the edge plasma. There is a rather large, inward net electromagnetic force (inward pinch velocity) in the H-mode phase of the discharge. There is a much smaller net electromagnetic force (pinch velocity) in the L-mode phase of the discharge. Thus, the outward pressure gradient forces must be larger in the H-mode phase than in the L-mode phase in order to satisfy momentum and particle balance constraints. The types of radial electric field and rotation profiles associated with this large inward pinch force

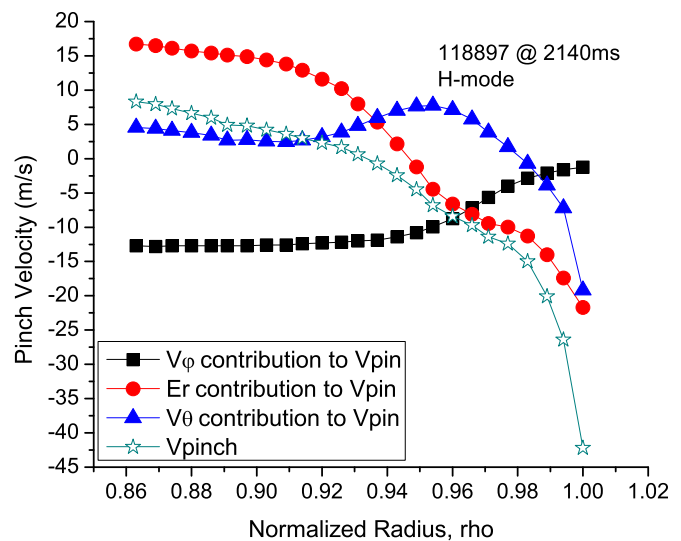


FIG. 10. (Color online) Inferred experimental pinch velocity in ELM-free H-mode phase of shot #118897.

have long been observed<sup>4</sup> but have in the past been interpreted in terms of shear stabilization of microinstability turbulence causing a reduction in the transport coefficients. The results of this paper suggest that it is a large increase in the inward pinch velocity, rather than a large decrease in diffusion coefficient, that characterizes the H-mode plasma edge relative to the L-mode. This insight suggests the possibility that a better understanding of the origin of the edge  $E_{\text{rad}}$  and poloidal rotation could lead to ways to control the pinch and in turn the edge density profile.

## ACKNOWLEDGMENTS

This work was supported by the U.S. Department of Energy under Grant No. DE-FG01-ER54538 with the Georgia Tech Research Corporation and by the U.S. Department of Energy under Contract No. DE-AC03-99ER54463 with General Atomics. The authors are grateful to other members of the DIII-D Team who took part in measuring and analyzing the data used in this paper. The first author appreciates the hospitality provided by General Atomics during part of this work.

## APPENDIX A: EVALUATION OF DEUTERIUM POLOIDAL ROTATION VELOCITY

In order to evaluate the collection of forces constituting the pinch velocity, it is necessary to evaluate the deuterium poloidal rotation velocity, which is not measured. We have set the deuterium poloidal velocity equal to the measured carbon poloidal velocity for this purpose in order to obtain a conservative lower bound on the magnitude of the pinch velocity (as explained in the following), even though there is theoretical and experimental evidence that the two velocities may be of different signs and magnitudes under certain conditions.

There are a number of multifluid models for the poloidal rotation velocity (many of them summarized in Ref. 31), all based on the poloidal momentum balance but with different assumptions of which terms must be retained and with different constitutive relations for friction and parallel viscosity coefficients evaluated from kinetic theory. The lead author and his colleagues have made numerous calculations of carbon and deuterium poloidal velocities over the years for models of DIII-D and other plasmas (e.g., Refs. 31–33). Two general conclusions emerge from these calculations. (1) In both the edge and the core, when the friction force is much less than the parallel viscous force, the deuterium and carbon ions rotate in opposite directions generally with different magnitudes, but when the friction force is greater than the viscous force, then both species rotate in the same direction with similar magnitudes. (2) In the plasma edge, the measured carbon rotation velocity is predicted (by the models described in Ref. 31 and the references therein) reasonably well in the flattop region but is significantly overpredicted in the steep-gradient region, probably indicating that a retarding torque (ion orbit loss? or viscous influx from SOL flows?) needs to be added to the model.

We note that the measurement of carbon and main ion poloidal rotation in a D-IIID helium plasma<sup>34</sup> (in which both

the main and impurity ion velocities can be measured) found the two species to be rotating in opposite directions. A calculation based on a trace-impurity limit of the Hirshman–Sigmar model (see Ref. 31), in which the viscosity term was neglected in the carbon equation, also predicted the two species rotating in different directions. However, these results cannot be generalized to other shots in DIII-D with different relative strengths of the parallel viscous and friction forces, as the calculations in Refs. 31–33 indicate.

For the shot examined in this paper, when the deuterium poloidal rotation term in the pinch velocity is evaluated using the measured carbon rotation velocity, its contribution to the pinch velocity reduces the contribution of the  $E_{\text{rad}}$  term. If the calculated deuterium rotation velocity, which is of the opposite sign, is used instead, the deuterium poloidal rotation term reinforces the  $E_{\text{rad}}$  term, leading to a much larger pinch velocity. Thus, we are left with the options of either (i) surely underestimating the effect on the pinch velocity by using the measured carbon velocity to evaluate the deuterium velocity term in the pinch velocity or (ii) using the calculated deuterium velocity (perhaps corrected for the difference in the measured and calculated carbon velocities) to evaluate the pinch velocity, which may significantly under- or overestimate the pinch velocity. We chose the first option in order to obtain a lower bound on the pinch velocity effect being investigated and to avoid the possibility of widely overestimating the pinch velocity effect.

- <sup>1</sup>G. L. Schmidt, S. Sesnic, R. Slusher, S. Suckewer, C. Surko, H. Takahashi, F. Tenney, H. Towner, and J. Valley, *J. Nucl. Mater.* **121**, 115 (1984).
- <sup>2</sup>M. Keilhacker, G. Becker, K. Bernhardt, A. Eberhagen, M. Elshaer, G. Fussman, O. Gehre, J. Genhardt, G. v. Gierke, E. Glock, G. Hass, F. Karger, S. Killel, O. Kluber, K. Knorrhett, K. Lackner, G. Lisitano, G. G. Lister, J. Massig, H. M. Mayer, K. McCormick, D. Meisel, I. Meservey, E. R. Muller, H. Murmann, H. Niedermeyer, W. Poschenedger, H. Rapp, B. Richter, H. Rohr, F. Ryter, F. Schneider, S. Siller, P. Smeulders, F. Soldner, E. Speth, A. Stabler, K. Steinmetz, K.-H. Steuer, Z. Szymanski, G. Venus, O. Vollmer, and F. Wagner, *Plasma Phys. Controlled Fusion* **26**, 49 (1984).
- <sup>3</sup>J. D. Callen, R. J. Groebner, T. H. Osborne, J. M. Canik, L. W. Owen, A. Y. Pankin, T. Rafiq, T. D. Rognlien, and W. M. Stacey, *Nucl. Fusion* **50**, 064004 (2010).
- <sup>4</sup>R. J. Groebner, K. H. Burrell, and R. P. Seraydarian, *Phys. Rev. Lett.* **64**, 3015 (1990).
- <sup>5</sup>W. M. Stacey and R. J. Groebner, *Phys. Plasmas* **15**, 012503 (2008).
- <sup>6</sup>W. M. Stacey and R. J. Groebner, *Phys. Plasmas* **16**, 102504 (2009).
- <sup>7</sup>L. A. Artsimovich, *Plasma Phys. Controlled Nucl. Fusion Res.* **2**, 595 (1966).
- <sup>8</sup>M. E. Rensink, S. L. Allen, A. H. Futch, D. N. Hill, G. D. Porter, and M. A. Mahdavi, *Phys. Fluids B* **5**, 2165 (1993).
- <sup>9</sup>J. Luxon, *Nucl. Fusion* **42**, 614 (2002).
- <sup>10</sup>W. M. Stacey and R. J. Groebner, *Phys. Plasmas* **14**, 012501 (2007).
- <sup>11</sup>R. J. Groebner, T. H. Osborne, A. W. Leonard, and M. E. Fenstermacher, *Nucl. Fusion* **49**, 045013 (2009).
- <sup>12</sup>C. F. Maggi, *Nucl. Fusion* **50**, 066001 (2010).
- <sup>13</sup>T. Onjun, G. Bateman, A. H. Kritiz, and G. Hammett, *Phys. Plasmas* **9**, 5018 (2002).
- <sup>14</sup>H. Urano, T. Takizuka, Y. Kamada, N. Oyama, H. Takenage, and JT-60 Team, *Nucl. Fusion* **48**, 045008 (2008).
- <sup>15</sup>T. H. Osborne, K. H. Burrell, R. J. Groebner, L. L. Lau, A. W. Leonard, R. Maingi, R. L. Miller, G. D. Porter, G. M. Stebler, and A. D. Turnbull, *J. Nucl. Mater.* **266–269**, 131 (1999).
- <sup>16</sup>C. F. Maggi, R. J. Groebner, C. Angioni, T. Hein, L. D. Horton, C. Konz, A. W. Leonard, C. C. Petty, A. C. C. Sips, P. B. Snyder, J. Candy, R. E. Waltz, ASDEX Upgrade, and DIII-D Teams, *Nucl. Fusion* **50**, 025023 (2010).

- <sup>17</sup>A. Kirk, T. O’Gorman, S. Saarelma, R. Scannell, H. R. Wilson, and MAST Team, *Plasma Phys. Controlled Fusion* **51**, 065016 (2009).
- <sup>18</sup>R. J. Groebner, P. B. Snyder, T. H. Osborne, A. W. Leonard, T. L. Rhodes, L. Zeng, E. A. Unterberg, Z. Yan, G. R. McKee, C. J. Lasnier, J. A. Boedo, and J. G. Watkins, *Nucl. Fusion* **50**, 064002 (2010).
- <sup>19</sup>H. R. Wilson, P. B. Snyder, G. T. A. Huysmans, and R. L. Miller, *Phys. Plasmas* **9**, 1277 (2002).
- <sup>20</sup>P. B. Snyder, H. R. Wilson, J. R. Ferron, L. L. Lao, A. W. Leonard, T. H. Osborne, A. D. Turnbull, D. Mossessian, M. Murakami, and X. Q. Xu, *Phys. Plasmas* **9**, 2037 (2002).
- <sup>21</sup>R. Scannell, A. Kirk, N. Bey Ayed, P. G. Carolan, G. Cunningham, J. McCone, S. L. Prunty, and M. J. Waslsh, *Plasma Phys. Controlled Fusion* **49**, 1431 (2007).
- <sup>22</sup>M. A. Beurskens, A. Alfier, B. Alper, I. Balboa, J. Flanagan, W. Fundamenski, E. Giovannozzi, M. Kernpenaars, A. Loarte, P. Lomas, E. de La Luna, I. Nunes, R. Pasqualotto, R. A. Pitts, G. Saibene, M. Walsh, S. Wiesen, and JET-EGDA Team, *Nucl. Fusion* **49**, 125006 (2009).
- <sup>23</sup>E. Wolfrum, A. Burchkhart, R. Fischer, N. Hicks, C. Konz, B. Kurzan, B. Langer, T. Putterich, H. Zohm, and ASDEX Upgrade Team, *Plasma Phys. Controlled Fusion* **51**, 124057 (2009).
- <sup>24</sup>A. Kojima, N. Oyama, Y. Sakamoto, Y. Kamada, H. Urano, K. Kamiya, T. Fujita, H. Kubo, N. Aiba, and JT-60 Team, *Nucl. Fusion* **49**, 115008 (2009).
- <sup>25</sup>N. Oyama, P. Gohil, L. D. Horton, A. E. Hubbard, J. W. Hughes, Y. Kamada, K. Kamiya, A. W. Leonard, A. Loarte, R. Maingi, G. Saibene, R. Sarton, J. K. Stober, W. Suttrop, H. Urano, W. P. West, and ITPA Pedestal Group, *Plasma Phys. Controlled Fusion* **48**, A171 (2006).
- <sup>26</sup>N. Oyama, A. Kojima, N. Aiba, L. D. Horton, A. Isayama, K. Kamiya, H. Urano, Y. Sakamoto, Y. Kamada, and JT-60 Team, *Nucl. Fusion* **50**, 064014 (2010).
- <sup>27</sup>J. Stober, P. J. Lomas, G. Saibene, Y. Andrew, P. Belo, G. D. Conway, A. Herrmann, L. D. Horton, M. Kempenaars, H.-R. Doslowski, A. Loarte, G. P. Maddison, M. Maraschek, D. C. McDonald, A. G. Meigs, P. Monier-Garbet, D. A. Mossessian, M. F. F. Nave, N. Oyama, V. Parail, Ch. P. Perez, F. Rimini, R. Sarton, A. C. C. Sips, P. R. Thomas, and JET-EFDA Team, *Nucl. Fusion* **45**, 1213 (2005).
- <sup>28</sup>G. Saibene, P. J. Lomas, R. Sartori, A. Loarte, J. Stober, Y. Andrew, S. A. Arshad, G. D. Conway, E. de La Luna, K. Gunther, L. C. Ingesson, M. A. H. Kempenaars, A. Korotkov, H. R. Koslowski, J. S. Lonnroth, D. C. McDonald, A. Meigs, P. Monier-Garbet, V. Parail, C. P. Perez, F. G. Rimini, S. Sharapov, and P. R. Thomas, *Nucl. Fusion* **45**, 297 (2005).
- <sup>29</sup>W. M. Stacey, *Phys. Plasmas* **15**, 052503 (2008).
- <sup>30</sup>W. M. Stacey, *Contrib. Plasma Phys.* **48**, 94 (2008).
- <sup>31</sup>W. M. Stacey, *Phys. Plasmas* **15**, 012501 (2008).
- <sup>32</sup>W. M. Stacey, *Phys. Fluids B* **4**, 3302 (1992).
- <sup>33</sup>W. M. Stacey, R. W. Johnson, and J. Mandrekas, *Phys. Plasmas* **13**, 062508 (2006).
- <sup>34</sup>J. Kim, K. H. Burrell, P. Gohill, R. J. Groebner, H. E. St. John, R. P. Seraydarian, and M. R. Wade, *Phys. Rev. Lett.* **72**, 2199 (1994).
- <sup>35</sup>K. H. Burrell, *Phys. Plasmas* **4**, 1499 (1997).
- <sup>36</sup>P. W. Terry, *Rev. Mod. Phys.* **72**, 109 (2000).